IEEE Access
Multidisciplinary | Rapid Review | Open Access Journal

Received March 1, 2018, accepted March 27, 2018, date of publication April 16, 2018, date of current version May 9, 2018.

Digital Object Identifier 10.1109/ACCESS.2018.2827021

Design and Analysis of a Series-Fed Aperture-Coupled Antenna Array With Wideband and High-Efficient Characteristics

MOHAMMAD MAHDI HONARI[1], (Student Member, IEEE), ABDOLALI ABDIPOUR[2], (Senior Member, IEEE), GHOLAMREZA MORADI[2], (Senior Member, IEEE), RASHID MIRZAVAND[1,2], (Senior Member, IEEE), AND PEDRAM MOUSAVI[1], (Senior Member, IEEE)

[1]Intelligent Wireless Technology Laboratory, University of Alberta, Edmonton, AB T6G 1H9, Canada
[2]Electrical Engineering Department, Amirkabir University of Technology, Tehran 15914, Iran

Corresponding author: Mohammad Mahdi Honari (honarika@ualberta.ca)

This work was supported by NSERC and AITF under the NSERC-AITF Industrial Chair Program.

ABSTRACT In this paper, a new wideband series-fed antenna array is proposed and analyzed. The antenna array structure consists of two antennas with two ports, two antennas with one port, and a wideband 180° coupler. A portion of power is propagated by the antenna with two ports, and the rest is propagated by the antenna with one port. A new wideband 180° coupler is designed in order to make the feed structure as compact as possible and to be integrated with the antenna array. Due to using elements with wideband structure, the overall antenna is wideband with measured bandwidth of 40% with reflection coefficient of 10 dB and 3 dB gain deviation from 3.85 to 5.75 GHz. The measured peak gain of 13.4 dBi has been achieved for the proposed 1×4 antenna array. The measured results shows that the efficiency is better than 87% and side lobe level at the frequencies of 4.6 and 5.4 GHz are, respectively, nearly -14 and -12 dB.

INDEX TERMS Aperture antenna, corrugated structures, dual-band antenna, substrate integrated waveguide.

I. INTRODUCTION

Nowadays planar antennas have extensively been used in many applications due to their light weight, relatively inexpensive price, low profile and ease of fabrication [1]–[3]. In this context, in recent years, considerable efforts have been devoted to solve some disadvantages of conventional planar structures, such as their low efficiency due to conductor and dielectric losses, narrow impedance bandwidth, relatively low gain, and poor polarization purity [4]–[7]. Although planar antennas can be used in systems with stringent requirements, they might present challenges especially in terms of efficiency for array antennas.

At the same time many attempts have put into increasing the bandwidth of the antenna, but this is still challenging in many application. Aperture coupled antennas may be a solution in wide bandwidth application due to their interesting characteristics such as isolating spurious feed radiation due to existence a ground plane between patch and feed line, in addition to wide bandwidth [8]–[11]. However, they have a low front to back ratio.

For array antenna structures, using corporate feeding network is a common approach in which a conventional Wilkinson power divider can be used to realize certain amplitudes of power to a single antenna. Although this technique allows the antenna array to have in-phase excitation of each element in a wide bandwidth, it has low efficiency due to dissipation losses within large feeding network [12]. In order to decrease the dissipation losses, a series feeding network can be utilized [13], [14]. This configuration in addition to providing simple and miniaturized feeding network [15], [16] enhances antenna efficiency, because the length of feeding network is significantly reduced with respect to conventional corporate feed counterparts [13]–[17]. Besides, it can reduce the unwanted coupling between radiating elements and feeding network [18]. Using series-fed antenna array structures causes a shift in radiation patterns versus frequency

which may cause a problem in some applications [19]–[21]. To avoid a beam tilt over a desired frequency range, an antenna array with two sides can be designed while both sides are excited by signals with the same amplitude and 180° phase difference over the range of frequency [22].

In this paper, design and analysis of a series-fed aperture coupled array is presented. Aperture coupled antennas provides relatively wide bandwidth. In addition, series feeding network provides high efficient and compact structure. The proposed antenna array is comprised of two antennas with two ports, two antennas with one port, and a wideband 180° coupler. All other components are designed to be wideband in order to have a wideband antenna array. The power entered into the antenna array is equally divided by two with 180° phase difference using an 180° coupler. The coupler is designed based on coupled line transmission lines which helps the structure to be compact and wideband. A portion of power is propagated into free space by the aperture coupled with two ports and the rest is propagated by the antenna with one port. Adjusting the transmitting power of antenna with two ports provides a control on peak gain and side lobe level. The measured reflection coefficient shows that an impedance matching is perfect over a large range of frequencies. Also, the maximum gain and efficiency of the antenna array are 13.4 dBi and 87% respectively. The side lobe level at the frequencies of 4.6 and 5.4 GHz are respectively about −14 and −12 dB.

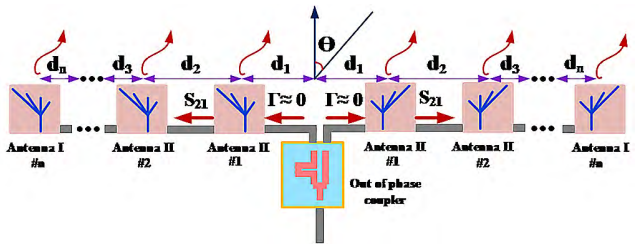

FIGURE 1. Block diagram of proposed structure.

II. ANTENNA CONFIGURATION AND DISCUSSION

The proposed compact and high efficient antenna is shown in Fig. 1. This configuration of series-fed antennas consists of 2n antenna elements which 2(n − 1) of them are two-port antennas (antenna II) and last antenna elements in both sides are one-port antenna (antenna I). Since the antenna array is fed from two symmetrical sides, an 180° coupler is needed in order to make the elements in-phase at both side of the array and keep the pattern at broadside direction over the operating bandwidth. The coupler divides the input signal between two ports with equal amplitude and 180° phase shift over the full operating bandwidth. When the signal enters antenna II, a portion of that is propagated by its radiator, and the rest is transmitted to its output port (second port) which is the input port of next element. This continues till last portion of signal is propagated by antenna I which has just one port.

It is possible to extract a circuit model for the antenna structure [23]–[25]. All two-port antennas can be considered as a two-port network with reflection coefficient, S_{11} and transmission, S_{21} responses. Inside each two-port network, some power is propagated into the space by the antenna. When the loss in the system is neglected, the power entered into each two-port network can be considered as reflected, transmitted to second port or propagated by the antenna element and thus we have,

$$S_{11}^2 + S_{21}^2 + A = 1, \tag{1}$$

which A is coupling propagation factor; the amount of power coupled to the antenna and propagated into the space. Further, when two-port network is designed to have no reflection (S_{11} = 0), the power entered either propagates or transmits to the second port, hence,

$$A = \sqrt{1 - S_{21}^2}. \tag{2}$$

Although (2) is correct when the loss and reflection coefficient are neglected, it provides a reasonable approximation. Using (2), the powers propagated by elements #1, #2, #3, ..., #(n − 1), #n are $\sqrt{1 - S_{21}^2}$, $S_{21}\sqrt{1 - S_{21}^2}$, $S_{21}^2\sqrt{1 - S_{21}^2}$, ..., $S_{21}^{(n-2)}\sqrt{1 - S_{21}^2}$, $S_{21}^{(n-1)}$, respectively. With the assumption of same radiator for antenna I and Antennas II, the array factor is obtained as,

$$\begin{aligned} |AF| = |&2\sqrt{1 - S_{21}^2}\cos(2\pi m_1 \cdot \sin\theta) \\ &+ 2S_{21}\sqrt{1 - S_{21}^2} \cdot e^{-j\alpha_2}\cos(2\pi(m_1 + m_2) \cdot \sin\theta) \\ &+ \ldots + 2S_{21}^{(n-2)}\sqrt{1 - S_{21}^2} \cdot e^{-j(\alpha_2+\alpha_3+\ldots+\alpha_{n-1})} \\ &\cos(2\pi(m_1 + m_2 + \ldots + m_{n-1}) \cdot \sin\theta) \\ &+ 2S_{21}^{(n-1)} \cdot e^{-j2\pi(\alpha_2+\ldots+\alpha_n)} \\ &\cos(2\pi(m_1 + m_2 + \ldots + m_{n-1} + m_n) \cdot \sin\theta)| \end{aligned} \tag{3}$$

which α_k is the phase delay that is occurred between antennas #k − 1 and #k, for k = 2, 3, ..., n and,

$$m_1 = \frac{d_1}{\lambda_g}, \quad m_2 = \frac{d_2}{\lambda_g}, \; m_3 = \frac{d_3}{\lambda_g}, \ldots, m_n = \frac{d_n}{\lambda_g} \tag{4}$$

An interesting result of (3) is that the array factor depends on transmission response of antennas II.

For the purpose of illustration, a four-element antenna array with centre frequency of 5 GHz is designed in this paper. In subsections below, the elements in proposed structure with 4 elements are discussed in detail.

A. COMPACT BROADBAND 180° COUPLER

A choice for 180° coupler can be a rat-race coupler. But, this coupler has large size and limited bandwidth [26]. Here, we propose an 180° coupler based on coupled lines phase shifter [27] and with broad bandwidth and relatively compact size. This coupler consists of a Wilkinson power divider and a proposed 180° Schiffman phase shifter. In [27], Schiffman proposed a broadband compact 90° phase shifter which mainly contains a coupled line and a single line as shown in Fig. 2(a). In this figure, Z_e and Z_o are respectively

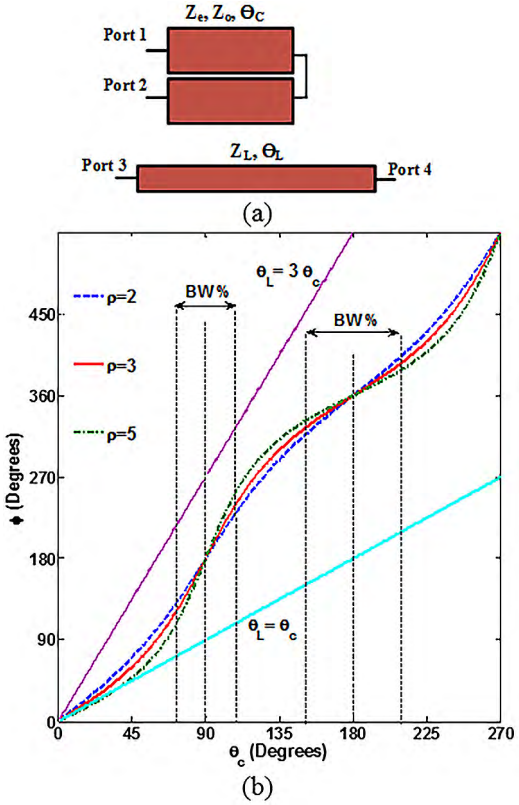

FIGURE 2. Schiffman phase shifter. (a) Structure and (b) Phase of coupled transmission line (phase of S_{21}).

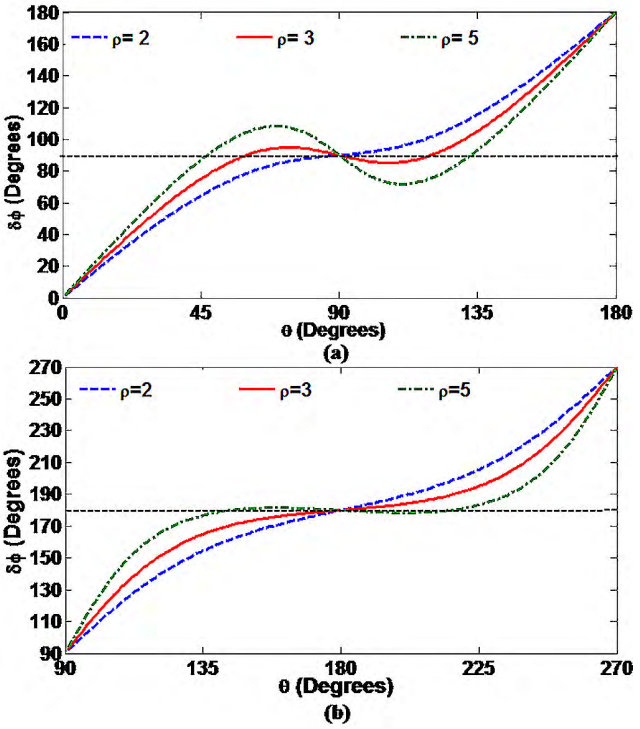

FIGURE 3. Phase difference response for (a) 90° Schiffman phase shifter [24] with K = 3, and (b) 180° proposed Schiffman phase shifter with K = 1.

even- and odd-mode characteristic impedances of coupled line and Z_L is impedance characteristic of single line. Also, θ_c and θ_L are electric lengths of coupled and single lines, respectively.

These phase shifters occupy small space and are broadband with simple structure. For general structure of Schiffman phase shifter shown in Fig. 2(a), the key parameters are $\theta_c = \lambda_0/4$, $\theta_L = 3\lambda_0/4$ which λ_0 is wavelength at center frequency. Furthermore, Z_e and Z_o are calculated in order to have a certain bandwidth or phase deviation, and input impedance of coupled transmission line [28]. Several references reported improvement in braodband 90° phase shifter [29]–[34]. Here, it is demonstrated that a simple coupled lines structure could result an 180° phase shift. For the coupled line, we have [27],

$$Z_I = \sqrt{Z_e Z_o} \tag{5}$$

$$\varphi = \cos^{-1}\left(\frac{\rho - \tan^2\theta_c}{\rho + \tan^2\theta_c}\right) \tag{6}$$

which

$$\rho = \frac{Z_e}{Z_o}. \tag{7}$$

In (5) and (6), Z_I and φ are input impedance and phase difference between ports 1 and 2 respectively. The phase shift is provided between ports 2 and 4 when ports 1 and 3 are excited with the same phase. Therefore, in Fig. 2(a) if $\theta_L = K\theta_c$, the phase shift is obtained as,

$$\delta\varphi = |K\theta_c - \cos^{-1}\left(\frac{\rho - \tan^2\theta_c}{\rho + \tan^2\theta_c}\right)|. \tag{8}$$

In (8), the phase shift consists of two terms for single and coupled lines. Fig. 2(b) shows ϕ in (6) for different ρ in terms of electrical length of coupled line. Also, for the single line, phase differences between ports 3 and 4 for K = 1, 3 are depicted. As shown, there is a zone near $\theta_c = 90°$ that phase difference between the line with K = 3 and a specific value of ρ is about 90 degrees. This is the mechanism of 90° Schiffman phase shifter. However, it can be seen that there is a zone near $\theta_c = 180°$ that phase difference between the line with K = 1 and a specific value of ρ is almost 180 degrees. These phase shifts described by (4) are presented in Fig. 3 for K = 3 and K = 1 which shows the phase difference responses for 90° and 180° phase shifters, respectively. As discussed before, for K = 3, we have 90° Schiffman phase shifter [27] shown in Fig. 3(a) that is based on (8). Furthermore, for K = 1, a phase shift of 180° can be obtained ($\theta_c = \theta_L = \lambda_0/2$). As shown, there is always a value of ρ that gives a certain phase deviation. It is quite evident that if we want a small phase deviation (more accurate phase shifter), the bandwidth will be lower.

The typical value of ρ for 90° phase shift depicted in Fig. 3(a) is lower than that of 180° phase shift proposed (Fig. 3(b)). The relatively high ρ for proposed

180° Schiffman phase shifter makes it hard to realize, because due to tight coupling, the gap between coupled lines becomes very small and requires a fairly expensive technology to fabricate. One solution is to select a thicker substrate that makes the gap bigger, but it affects the performance of other circuits in the system. Alternative solution is to use multi-section coupled lines instead of one coupled line that their total length is the length of the original coupled line ($\theta_c = \lambda_0/2$) [34]. This not only gives more freedom for the design, but also provides wider bandwidth. Furthermore, this approach allows the designer to select a realizable gap between coupled lines. Because of using different length and width for transmission lines, it could match the impedance as well to make the coupler broadband.

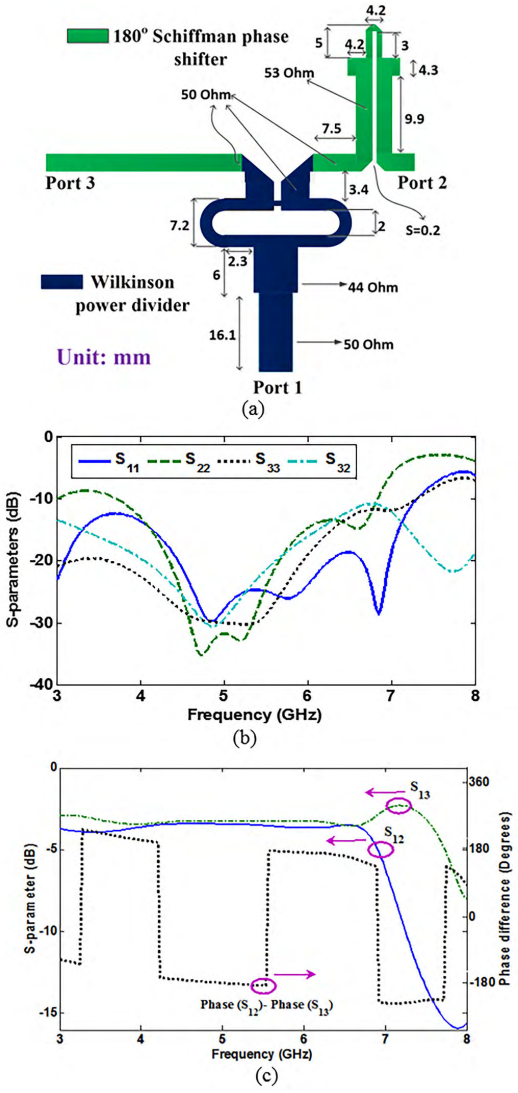

FIGURE 4. Out of phase coupler, (a) Schematic, (b) Simulated S-parameter of proposed 180° coupler and (c) Simulated S-parameter and phase difference between output ports of proposed 180° coupler.

Fig. 4(a) shows the schematic of 180° coupler. It consists of an 180° coupled lines phase shifter and Wilkinson power divider. This coupler is designed on Rogers RT/Duroid 5880 with relative permittivity of 2.2 and loss tangent of 0.0009. The optimized dimensions are shown in Fig. 4(a). Because of the manufacturing limitation, the gap between coupled lines is selected to be 0.2 mm. Port 1 is the input port and ports 2 and 3 are the output ports which have the same amplitude and 180° phase shift at operating bandwidth. The simulated matching and isolation responses have been depicted in Fig. 4(b) which prove the wideband nature of the proposed coupler. As shown in Fig. 4(c), the transmission responses about 3.4±0.2 dB have been obtained for two output ports in the desired bandwidth which are satisfactory. Furthermore, a phase difference of almost 180±10 degrees has been achieved for 4-6 GHz range. This accuracy is enough for the antenna array; however, it can be improved by more optimization or making the gap between coupled lines smaller.

B. TWO PORT ANTENNA DESIGN AND DISCUSSION

In the proposed antenna with 4 elements, the approximate array factor will be,

$$|AF| = |2\sqrt{1 - S_{21}^2}\cos(2\pi m_1 \cdot \sin\theta) + 2S_{21}e^{-j\alpha_2}\cos(2\pi(m_1 + m_2)\cdot\sin\theta)| \quad (9)$$

The length of transmission line between antennas I and II is selected such that the delay $\alpha_2 = 2\pi$. To have the maximum gain at broadside ($\theta = 0$), the maximum value of AF is obtained for $S_{21} = 0.707$. However, it was expected because to have maximum gain, the array has to be a uniform array and all elements must have the same weight (amplitude and phase).

To reduce side lobe level, the distribution of amplitude of the elements has to follow Dolph-Chebyshev array. To have a side lobe level of −15 dB for a 4 element array antenna, the amplitude distribution of the elements are calculated to be 1.33 for Antennas II and 1 for antenna I in the configuration proposed in Fig. 1. This means that if the radiators are the same, antenna II and antenna I propagate 64% and 36% of the whole power based on proposed configuration which corresponds to transmission response of almost −4.5 dB for antenna II. In this case, the maximum gain decreases. As a conclusion, when the transmission response is near −3 dB, the peak gain is maximum although the side lobe level is not minimum and when it is almost −4.5 dB, the side lobe level is about −15 dB which is very good for 4 element array antenna. For other values of transmission response between −3 to −4.5 dB, there is a trade-off between the peak gain and side lobe level. The goal would be to keep the transmission response of the antenna II between almost −3 to −4.5 dB in the desired bandwidth to have an array antenna with a low side lobe level and the highest possible gain, while it is designed to be wideband.

Due to broadband characteristics of the aperture-coupled antenna, it is employed for the antennas elements. Besides, aperture-coupled antennas provide more degree of freedom to optimize at the expense of a small complication in the design.

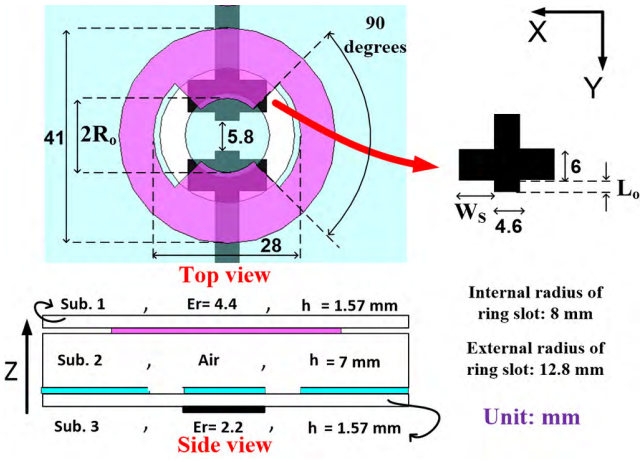

FIGURE 5. The proposed antenna configuration as antenna II.

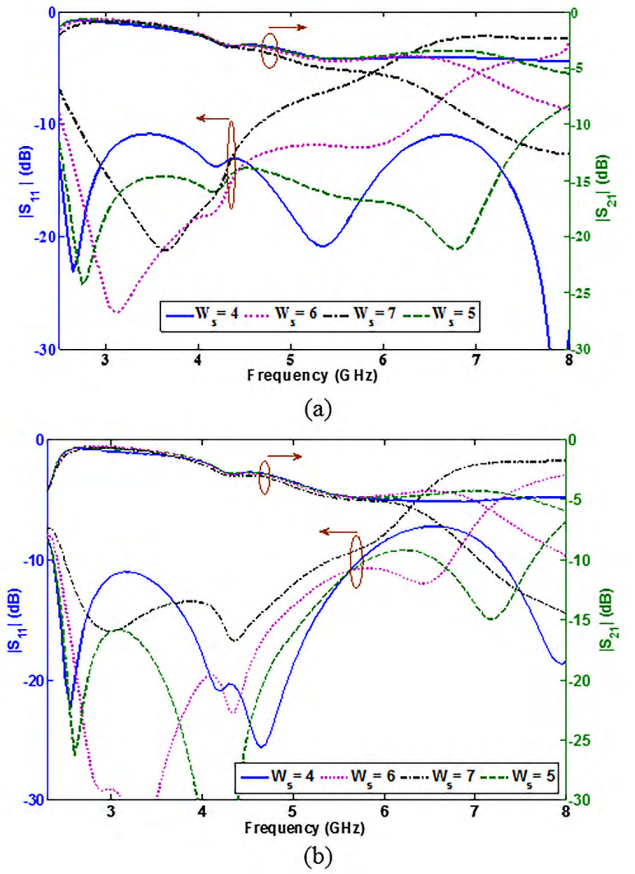

FIGURE 6. The effect of varying W_S on the reflection coefficient and transmission response of antenna II with $R_O = 11$mm, (a) $L_O = 1.55$, and (b) $L_O = 0.55$ mm.

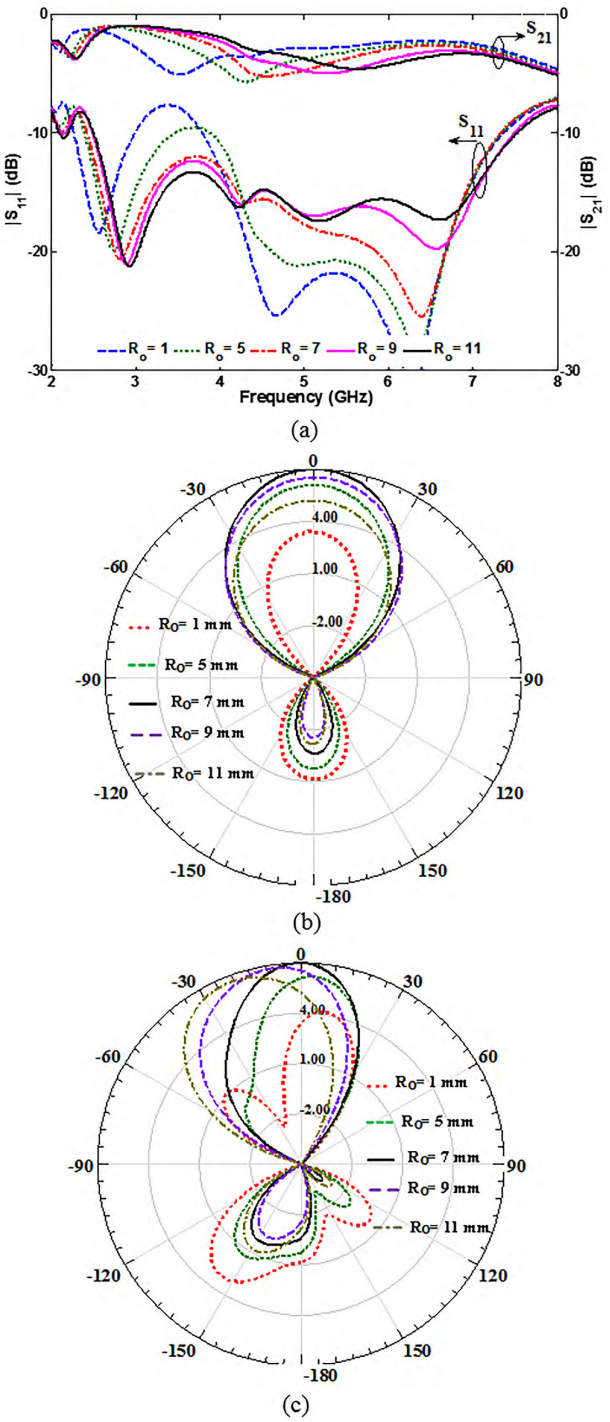

FIGURE 7. The effect of varying R_O with $L_O = 1.6$ mm and $W_S = 5.2$ mm on (a) the reflection coefficient and the transmission response, (b) H-plane at 5 GHz, and (c) E-plane at 5 GHz of antenna II.

For designing antenna II, three factors have to be considered. First, the patch configuration has to be designed appropriately in order to make a good radiation pattern and sufficient gain. The configuration of patch also affects reflection coefficient which needs to be accounted for. Second, the shape of feed line is an important issue in the design because it mainly controls the reflection and transmission responses of antenna II. Last, the slot created in ground plane should be resonant in center frequency.

The proposed configuration for antenna II is shown in Fig. 5. As indicated, it is an aperture-coupled antenna consisted of the input and output port feed lines, the ring slot, and

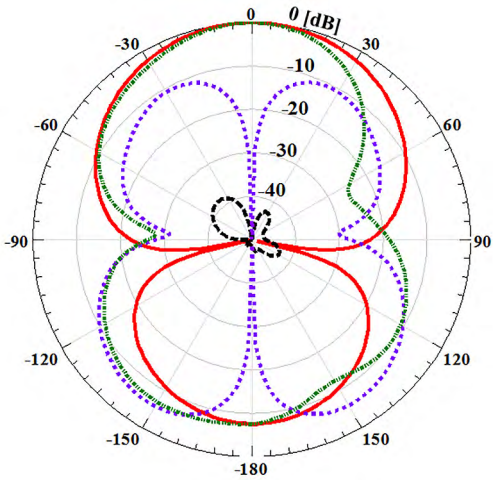

FIGURE 8. Radiation pattern of antenna II at 5 GHz.

the ring patch. A portion of the power entered from input feed line is coupled to the patch through ring slot and propagates and the rest is coupled to output feed line to reach antenna I. The transmission response, reflection coefficient response and radiation characteristics of the proposed antenna array can be controlled by the shape and dimensions of the feed lines, slot, and patch.

In the proposed structure for antenna II as shown in Fig. 5, a ring slot with the inner radius of 8 mm and outer radius of 12.8 mm is designed to make a resonance around 5 GHz. This three-layer antenna consists of a FR4 substrate with relative permittivity of 4.4 and thickness of 1.57 mm as top layer, and a Rogers RT/Duroid 5880 substrate (we used the same substrate for the coupler) with relative permittivity of 2.2 and thickness of 1.57 mm as the bottom layer. There is a 7 mm air gap between top and bottom layers. A cross shape feed line is selected to give more degrees of freedom for adjusting the reflection coefficient and the transmission response. A segmented ring patch is designed such that it could provide appropriate radiation pattern and gain.

Two parameters L_O and W_S of feed line, shown in Fig. 5, mainly affect the reflection coefficient and the transmission response while R_O mostly adjusts the radiation pattern and the peak gain of antenna II. The effect of L_O and W_S on :$|S_{21}|$ and $|S_{11}|$of antenna II is depicted in Fig. 6. It is observed that by adjusting the feed line dimensions, it is possible to obtain a suitable reflection coefficient ($|S_{11}| < -10$ dB) and a desired transmission response (-4.5 dB $< |S_{21}| < -3$ dB) simultaneously. The effect of R_O on reflection coefficient, transmission response, and radiation patterns and peak gain is shown in Fig. 7. It can be seen that for some values of R_O, not only the reflection coefficient and transmission response are in the desired range over a wide range of frequencies including the center frequency at 5 GHz, but also the radiation pattern and especially the peak gain improves. Based on optimization of these parameters, the final values are $L_O = 1.6$ mm, $W_S = 5.2$ mm, and $R_O = 7$ mm.

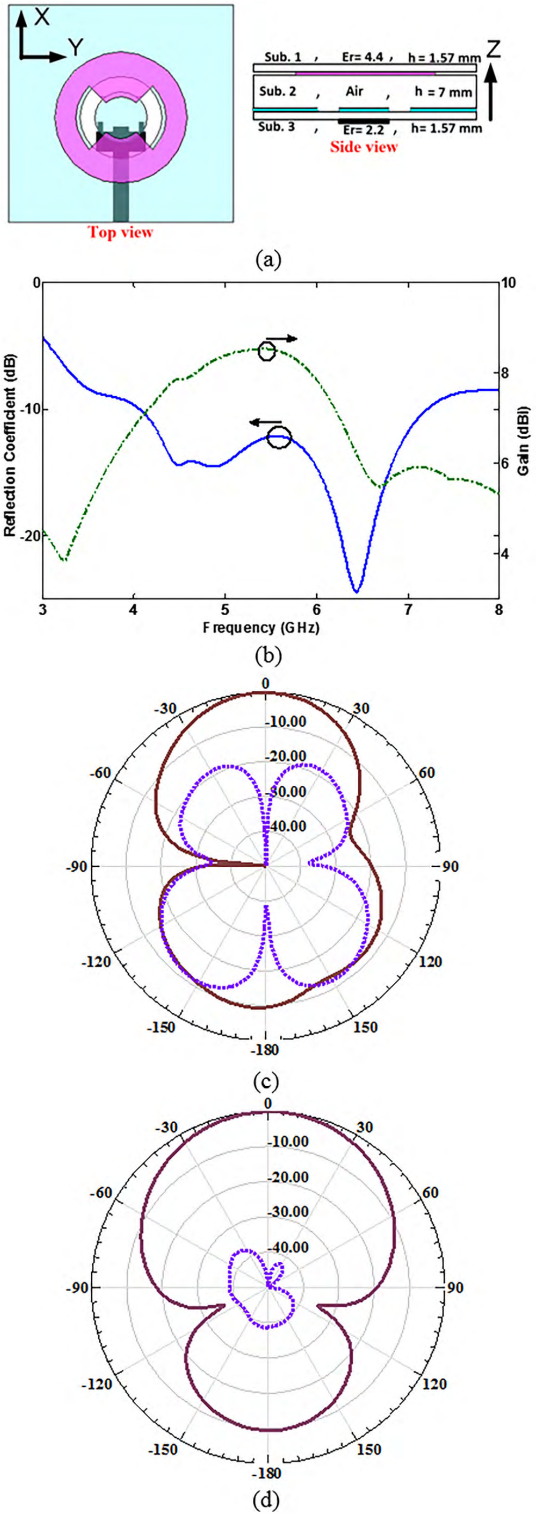

FIGURE 9. One port antenna, (a) proposed structure, (b) Reflection coefficient and gain, (c) Simulated co-polarization (Solid line) and cross-polarization (dot line) of E-plane at 5 GHz, and (d) Simulated co-polarization (Solid line) and cross-polarization (dot line) of H-plane at 5 GHz.

For these values, the reflection coefficient is better than -10 dB over 2.4-7.2 GHz and the transmission response is between -3 to -4.8 dB over 3.8-6.1 GHz, as shown

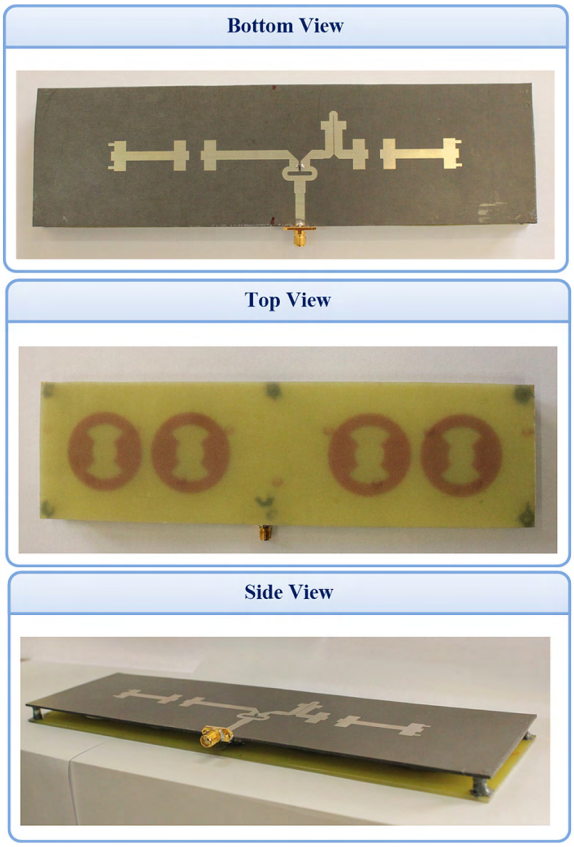

FIGURE 10. Different views of fabricated antenna (bottom, top, and side views).

in Fig. 7(a). This variation over the frequency band is acceptable. The peak gain of the antenna is also about 7 dBi at 5 GHz for the optimum values achieved. Fig. 8 depicts the radiation patterns of antenna II which shows the antenna is linearly polarized with a cross-polarization of better than 10 dB in half power beamwidth for both planes.

C. ONE-PORT ANTENNA DESIGN AND DISCUSSION

In this subsection, the design procedure of the antenna I as shown in Fig. 1 is considered. This antenna propagates the rest of the power coming from output port of antenna II. Fig. 9(a) shows the antenna I's configuration. The structure is similar to antenna II with one of the feed lines is removed and R_O is reduced to 6.5 mm. Furthermore, to have a better reflection coefficient, two small rectangular patches have been added to the end of feed line as shown in Fig. 9(a). The reflection coefficient and peak gain of the antenna I are depicted in Fig. 9(b). It is seen that a peak gain of more than 7 dBi is achieved over the wide frequency range with a reflection coefficient better than −10 dB. Figs. 9(c) and 9(d) show the radiation patterns of antenna I at the center frequency which illustrates a good linear polarization. The simulated cross-polarization level in the half power beamwidth is at least 19 dB below the co-polarization in the E-plane and almost 37 dB below the co-polarization in the H-plane.

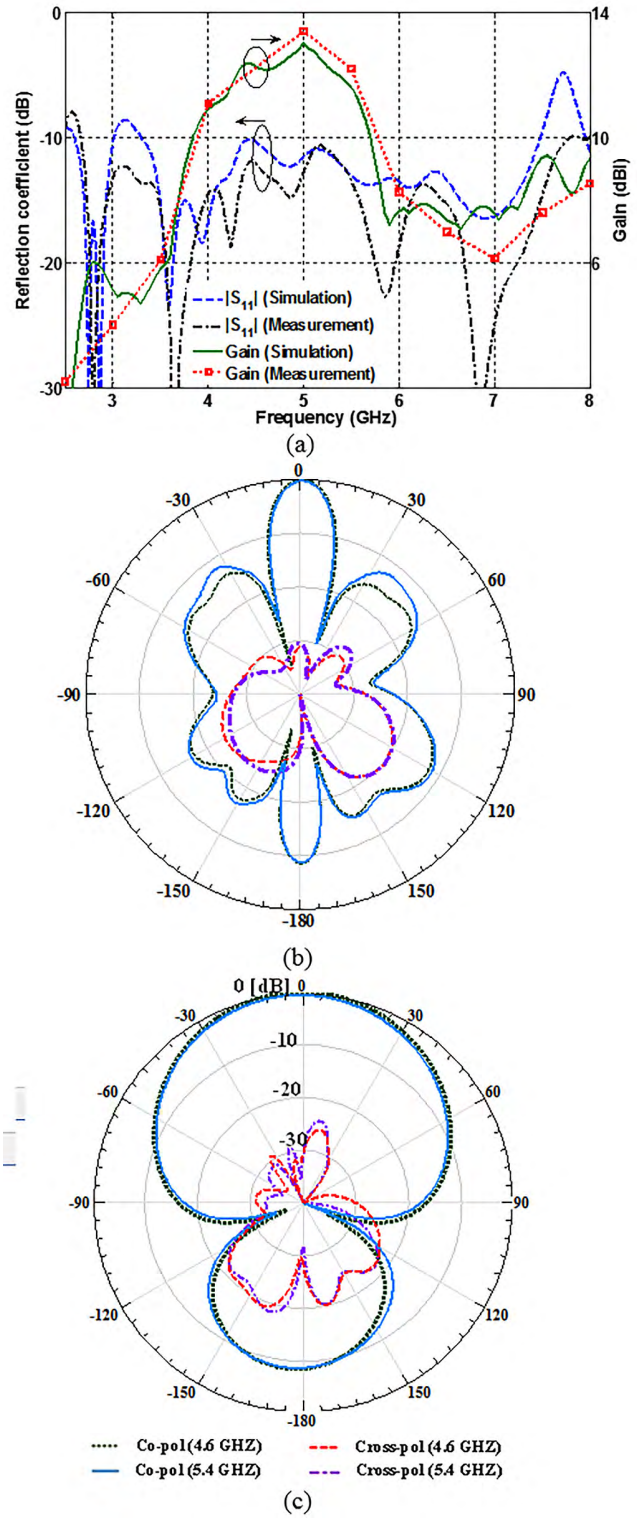

FIGURE 11. (a) Reflection coefficient and peak gain of the proposed antenna array, (b) the measured radiation pattern of the proposed antenna array at the frequencies of 4.6 and 5.4 GHz in E-plane, (c) the measured radiation pattern of the proposed antenna array at the frequencies of 4.6 and 5.4 GHz in H-plane.

III. MEASUREMENT RESULTS

A prototype of the proposed array antenna has been fabricated as shown in Fig. 10. In the bottom view, the 180° coupler

and feed lines for one-port and two-port antennas can be seen. Four ring patches are also shown in the top view of the array antenna. The separation between FR4 and RT Doroid substrates is fixed using spacers at the four corners of substrates. The reflection coefficient of the fabricated antenna is measured using an Agilent-8722ES vector network analyzer. The simulated and measured reflection coefficient and peak gain are displayed in Fig. 11(a) which are in agreement. The measured reflection coefficient shows an impedance matching ($|S11| < -10$ dB) of 97% from 2.7 to 7.8 GHz. The coupling mechanism used in the antenna structures helped to achieve a wideband impedance bandwidth. The measured peak gain at center frequency is about 13.4 dBi as shown in Fig. 10(a) which is considered a relatively high gain for four element array.

A standard far-filed antenna test has been used for the pattern test of the proposed antenna array. As a source antenna, a conventional horn antenna has been employed which was 6 meter away from the antenna array in an anechoic chamber. Figs. 10(b) and 10(c) illustrate the measured E- and H-plane radiation patterns of the array antenna at 4.6 and 5.4 GHz. The major different between these frequencies is the amount of side lobe level (SLL). At the frequency of 4.6 GHz, SLL is about -14 dB; however, this parameter for the frequency of 5.4 GHz is almost -12 dB. For both frequencies in E- and H-planes, the cross-polarizations in the half power beanwidth are at least 24 dB below their co-polarizations which shows the extreme linearity of the fabricated antenna. The measured efficiency of the antenna is better that 87% over the desired frequency band. It is possible to use more elements in the proposed array configuration, if more directive antenna is needed. The proposed antenna design technique can be used in many wideband applications and multi-standard wireless communication systems which needs wide bandwidth.

IV. CONCLUSION

The design procedure and analysis of a wideband series-fed antenna array has been proposed in detail. For wideband response, each of the antenna elements and 180° coupler was designed to be wideband. The series feeding network makes the structure compact and efficient. The results showed that the proposed 1×4 antenna array has great characteristics such as high gain and efficiency, very low cross-polarization, relatively low side lobe level, and wide bandwidth. Our proposed technique for designing this antenna array can be extended to design an antenna array with more elements. Also, it is possible to use this antenna array as a sub-array in a larger array antenna. The antenna can be used in many wideband application and multi-standard wireless communication systems.

REFERENCES

[1] J. Li, Q. Zeng, R. Liu, and T. A. Denidni, "A gain enhancement and flexible control of beam numbers antenna based on frequency selective surfaces," *IEEE Access*, vol. 6, pp. 6082–6091, 2018.

[2] M. M. Honari, R. Mirzavand, H. Saghlatoon, and P. Mousavi, "A dual-band low-profile aperture antenna with substrate-integrated waveguide grooves," *IEEE Trans. Antennas Propag.*, vol. 64, no. 4, pp. 1561–1566, Apr. 2016.

[3] F. M. Monavar, S. Shamsinejad, R. Mirzavand, J. Melzer, and P. Mousavi, "Beam-steering SIW leaky-wave subarray with flat-topped footprint for 5G applications," *IEEE Trans. Antennas Propag.*, vol. 65, no. 3, pp. 1108–1120, Mar. 2017.

[4] K. Da Xu, H. Xu, Y. Liu, J. Li, and Q. H. Liu, "Microstrip patch antennas with multiple parasitic patches and shorting vias for bandwidth enhancement," *IEEE Access*, vol. 6, pp. 11624–11633, 2018.

[5] M. M. Honari, R. Mirzavand, J. Melzer, and P. Mousavi, "A new aperture antenna using substrate integrated waveguide corrugated structures for 5G applications," *IEEE Antennas Wireless Propag. Lett.*, vol. 16, pp. 254–257, 2017.

[6] W. El-Halwagy, R. Mirzavand, J. Melzer, M. Hossain, and P. Mousavi, "Investigation of wideband substrate-integrated vertically-polarized electric dipole antenna and arrays for mm-Wave 5G mobile devices," *IEEE Access*, vol. 6, pp. 2145–2157, 2018.

[7] H. Aliakbari, A. Abdipour, A. Costanzo, D. Masotti, R. Mirzavand, and P. Mousavi, "ANN-based design of a versatile millimetre-wave slotted patch multi-antenna configuration for 5G scenarios," *IET Microw., Antennas Propag.*, vol. 11, no. 9, pp. 1288–1295, 2017.

[8] A. Gupta and R. K. Gangwar, "Dual-band circularly polarized aperture coupled rectangular dielectric resonator antenna for wireless applications," *IEEE Access*, vol. 6, pp. 11388–11396, 2018.

[9] Q. Fang, L. Song, M. Jin, Y. Han, and X. Qiao, "Dual polarised aperture-coupled patch antenna using asymmetrical feed," *IET Microw. Antennas Propag.*, vol. 9, no. 13, pp. 1399–1406, 2015.

[10] M. M. Honari, A. Abdipour, and G. Moradi, "Bandwidth and gain enhancement of an aperture antenna with modified ring patch," *IEEE Antennas Wireless Propag. Lett.*, vol. 10, pp. 1413–1416, 2011.

[11] V. P. Sarin, M. S. Nishamol, D. Tony, C. K. Aanandan, P. Mohanan, and K. Vasudevan, "A wideband stacked offset microstrip antenna with improved gain and low cross polarization," *IEEE Trans. Antennas Propag.*, vol. 59, no. 4, pp. 1376–1379, Apr. 2011.

[12] I. Slomian, K. Wincza, and S. Gruszczynski, "Compact integrated feeding network for excitation of dual-circular polarization in series-fed antenna lattice," *IEEE Trans. Antennas Propag.*, vol. 62, no. 11, pp. 5876–5879, Nov. 2014.

[13] G.-L. Huang, S.-G. Zhou, T.-H. Chio, C.-Y.-D. Sim, and T.-S. Yeo, "Waveguide-stripline series–corporate hybrid feed technique for dual-polarized antenna array applications," *IEEE Trans. Compon. Packag. Manuf. Technol.*, vol. 7, no. 1, pp. 81–87, Jan. 2017.

[14] H.-L. Kao *et al.*, "Inkjet printed series-fed two-dipole antenna comprising a balun filter on liquid crystal polymer substrate," *IEEE Trans. Compon., Packag., Manuf. Technol.*, vol. 4, no. 7, pp. 1228–1236, Jul. 2014.

[15] A. Bisognin *et al.*, "Differential feeding technique for mm-wave series-fed antenna-array," *Electron. Lett.*, vol. 49, no. 15, pp. 918–919, Jul. 2013.

[16] Y.-B. Jung, I. Yeom, and C. W. Jung, "Centre-fed series array antenna for K-/Ka-band electromagnetic sensors," *IET Microw. Antennas Propag.*, vol. 60, no. 6, pp. 588–593, 2012.

[17] A. A. Vallecchi and G. B. Gentili, "Design of dual-polarized series-fed microstrip arrays with low losses and high polarization purity," *IEEE Trans. Antennas Propag.*, vol. 53, no. 5, pp. 1791–1798, May 2005.

[18] C. Min and C. E. Free, "Analysis of circularly polarised dual-ring microstrip patch array using hybrid feed," *IET Microw. Antennas Propag.*, vol. 3, no. 3, pp. 465–472, 2009.

[19] M. Yousefbeigi, A. Enayati, M. Shahabadi, and D. Busuioc, "Parallel–series feed network with improved G/T performance for high-gain microstrip antenna arrays," *IET Electron. Lett.*, vol. 44, no. 3, pp. 180–182, 2008.

[20] J. A. Vitaz, A. M. Buerkle, and K. Sarabandi, "Tracking of metallic objects using a retro-reflective array at 26 GHz," *IEEE Trans. Antennas Propag.*, vol. 58, no. 11, pp. 3539–3544, Nov. 2010.

[21] F.-Y. Kuo and R.-B. Hwang, "High-isolation X-band marine radar antenna design," *IEEE Trans. Antennas Propag.*, vol. 62, no. 5, pp. 2331–2337, May 2014.

[22] X. M. Zhang, J. L. Huyan, P. C. Gao, H. Wang, and Y. F. Zheng, "Stacked series-fed linear array antenna with reduced sidelobe," *IET Electron. Lett.*, vol. 50, no. 4, pp. 251–253, 2014.

[23] W. M. Abdel-Wahab, D. Busuioc, and S. Safavi-Naeini, "Millimeter-wave high radiation efficiency planar waveguide series-fed dielectric resonator antenna (DRA) array: Analysis, design, and measurements," *IEEE Trans. Antennas Propag.*, vol. 59, no. 8, pp. 2834–2843, Aug. 2011.

[24] M. Abdallah, Y. Wang, W. M. Abdel-Wahab, and S. Safavi-Naeini, "A tunable circuit model for the modeling of dielectric resonator antenna array," *IEEE Antennas Wireless Propag. Lett.*, vol. 15, pp. 830–833, 2016.

[25] I. Mohamed and A. R. Sebak, "High-gain series-fed aperture-coupled microstrip antenna array," *Mirow. Opt. Technol. Lett.*, vol. 57, no. 1, pp. 91–94, 2015.
[26] M. M. Honari, R. Mirzavand, P. Mousavi, and A. Abdipour, "Class of miniaturised/arbitrary power division ratio couplers with improved design flexibility," *IET Microw. Antennas Propag.*, vol. 9, no. 10, pp. 1066–1073, 2015.
[27] B. M. Schiffman, "A new class of broad-band microwave 90-degree phase shifters," *IRE Trans. Microw. Tech.*, vol. 6, no. 2, pp. 232–237, Apr. 1958.
[28] J. L. R. Quirarte and J. P. Starski, "Novel Schiffman phase shifters," *IEEE Trans. Microw. Theory Techn.*, vol. 41, no. 1, pp. 9–14, Jan. 1993.
[29] Y.-X. Guo, Z.-Y. Zhang, and L. Ong, "Improved wide-band Schiffman phase shifter," *IEEE Trans. Microw. Theory Techn.*, vol. 54, no. 3, pp. 1196–1200, Mar. 2006.
[30] Q. Liu, H. Liu, and Y. Liu, "Compact ultra-wideband 90° phase shifter using short-circuited stub and weak coupled line," *IET Electron. Lett.*, vol. 50, no. 20, pp. 1454–1456, 2014.
[31] R. Mirzavand, B. Honarbakhsh, A. Abdipour, and A. Tavakoli, "Metamaterial-based phase shifters for ultra wide-band applications," *J. Electromagn. Waves Appl.*, vol. 23, nos. 11–12, pp. 1489–1496, 2009.
[32] M. M. Honari, R. Mirzavand, and P. Mousavi, "Design of wideband phase shifters with low phase error using parallel inductor and capacitor for wideband antenna applications," *J. Electromagn. Waves Appl.*, vol. 31, no. 7, pp. 716–726, 2017.
[33] C. E. Free and C. S. Aitchison, "Improved analysis and design of coupled-line phase shifters," *IEEE Trans. Microw. Theory Techn.*, vol. 43, no. 9, pp. 2126–2131, Sep. 1995.
[34] V. P. Meschanov, I. V. Metelnikova, V. D. Tupikin, and G. G. Chumaevskaya, "A new structure of microwave ultrawide-band differential phase shifter," *IEEE Trans. Microw. Theory Techn.*, vol. 42, no. 5, pp. 762–765, May 1994.

MOHAMMAD MAHDI HONARI (S'14) received the B.Sc. degree from the Ferdowsi University of Mashhad, Mashhad, Iran, and the M.Sc. degree from the Amirkabir University of Technology, Tehran, Iran.

He is currently pursuing the Ph.D. degree with the Intelligent Wireless Technology Laboratory, University of Alberta, Edmonton, Canada. His research areas include RF/microwave/mm-wave circuits, broadband active integrated antennas, phased array antennas, sensors, and metamaterial.

Dr. Honari received the Best M.Sc. Researcher Award in telecommunications and the Best M.Sc. Thesis Award from the Amirkabir University of Technology in 2012. He is a recipient of the Alberta Innovates Technology Futures Ph.D. Scholarship from 2015 to 2018.

ABDOLALI ABDIPOUR (M'97–SM'06) was born in Alashtar, Iran, in 1966. He received the B.Sc. degree in electrical engineering from Tehran University, Tehran, Iran, in 1989, the M.Sc. degree in electronics from the University of Limoges, Limoges, France, in 1992, and the Ph.D. degree in electronics engineering from the University of Paris XI, Paris, France, in 1996. He is currently a Professor with the Department of Electrical Engineering, Amirkabir University of Technology, Tehran. He has authored five books and authored or co-authored over 300 papers in refereed journals and local and international conferences. His current research interests include wireless communication systems (RF technology and transceivers), RF/Microwave/mm-wave/terahertz circuit and system design, the electromagnetic modeling of active devices and circuits, high-frequency electronics (signal and noise), nonlinear modeling, and the analysis of microwave devices and circuits.

GHOLAMREZA MORADI (M'09–SM'16) was born in Shahriar, Iran, in 1966. He received the B.Sc. degree in electrical communication engineering from Tehran University, Tehran, Iran, in 1989, the M.Sc. degree in electrical communication engineering from the Iran University of Science and Technology, Tehran, in 1993, and the Ph.D. degree in electrical engineering from Tehran Polytechnic University, Tehran, in 2002. From 1997 to 2006, he was a Faculty Member with the Civil Aviation Technology College, Tehran. In 2003, he was selected as an Exemplary Researcher of the Iranian Ministry of Road and Transportation. He is currently an Associate Professor with the Department of Electrical Engineering, Amirkabir University of Technology (Tehran Polytechnic), Tehran. He has authored or co-authored several papers in refereed journals and local and international conferences. He has co-authored *Communication Transmission Lines* [Nahr-e-Danesh Press, 2007 (in Persian)], *Active Transmission Lines* [Amirkabir University Press, 2008 (in Persian)], and *Microwave Engineering* [Nahr-e-Danesh Press, 2008 (in Persian)]. His main research interests include numerical electromagnetics, antennas, and active microwave and millimeter-wave circuits and systems.

RASHID MIRZAVAND (M'12–SM'16) received the B.Sc. degree from the Isfahan University of Technology, Isfahan, Iran, in 2004, and the M.Sc. and Ph.D. degrees from the Amirkabir University of Technology (Tehran Polytechnic), Tehran, Iran, in 2007 and 2011, respectively, all in electrical engineering.

Since 2011, he has been a Research Professor with the Amirkabir University of Technology. He is currently a Research Associate with the Intelligent Wireless Technology Laboratory, University of Alberta, Edmonton, AB, Canada. He has authored of over 100 papers published in refereed journals and conferences proceedings. His research interests include integrated sensors and microwave/millimeter-wave circuits.

Dr. Mirzavand received the Best Ph.D. Thesis Award from the Amirkabir University of Technology in 2012, the Best National ICT Researcher Award from the Ministry of Information and Communications Technology of Iran in 2013, the Elite Young Researcher Grant Award from Iran's NEF in 2014, and the Alberta Innovates Technology Futures Elite Postdoctoral Fellowship Award in 2015.

PEDRAM MOUSAVI (M'00–SM'14) received the B.Sc. degree in telecommunication engineering from the Iran University of Science and Technology, Tehran, Iran, in 1995, and the M.Sc. and Ph.D. degrees in electrical engineering from the University of Manitoba, Winnipeg, MB, Canada, in 1997 and 2001, respectively.

He is currently an Associate Professor with the Department of Mechanical Engineering and the Department of Electrical and Computer Engineering and the NSERC-AITF Industrial Research Chair in intelligent integrated sensors and antennas with the University of Alberta, Edmonton, AB, Canada. He has over 15 years of entrepreneurial academic experience with startup companies from the University of Waterloo and the University of Alberta. His research interests include advanced intelligent antennas, microwave/millimeter-wave circuits and systems, UWB radar systems, and 3-D printing electronics. He has published over 150 refereed journal and conference articles and holds several patents in his fields of research. His current mission is to foster a strong collaboration between industry and academia.